

## Critical form and feedbacks in mountain-belt dynamics: Role of rheology as a tectonic governor

Gerard H. Roe<sup>1</sup> and Mark T. Brandon<sup>2</sup>

Received 27 April 2009; revised 30 August 2010; accepted 11 October 2010; published 4 February 2011.

[1] The rheology that governs deformation within a convergent orogen also controls its topographic form, or in other words, the covariation of its height (or thickness) and its width. Under conditions pertaining to small orogens and for rheologies ranging from linear viscous to Coulomb plastic, we show that this topographic form is insensitive to the distributions of fluxes into and out of the wedge and is thus a fundamental property of the system. It can therefore be thought of as a “critical” topographic form, directly analogous to the well-studied case of a Coulomb plastic rheology, which predicts a constant critical taper angle, independent of its size. The tendency of the system to evolve toward a critical topographic form can be regarded as a “tectonic governor” that strongly damps the response of the orogen to changes in climate or tectonic forcing. Scaling relationships can be derived for the variation of orogen width, height, and exhumation rate as a function of accretionary flux and precipitation rate. This study explores how sensitive these scaling relationships are to the assumed rheology. It is found that the scaling relationships vary by less than a factor of 2 across the range of typical geological rheologies, from Coulomb friction, to power law viscous, to linear viscous. These scaling relationships provide a first-order representation of the behavior of convergent wedges and are relatively insensitive to the underlying assumptions.

**Citation:** Roe, G. H., and M. T. Brandon (2011), Critical form and feedbacks in mountain-belt dynamics: Role of rheology as a tectonic governor, *J. Geophys. Res.*, 116, B02101, doi:10.1029/2009JB006571.

### 1. Introduction

[2] For as long as the Earth Sciences have been studied, a major goal has been to understand what controls the fundamental attributes of a mountain range, such as height, width, and the pattern and magnitude of the internal deformation. At the broadest level, the challenge reduces to characterizing the relative importance of tectonic, erosional, and climatic processes, the combination of which must ultimately be controlling the orogenic system. While these questions are important to many individual disciplines, research has tended to approach the challenge from different perspectives. For example, many geomorphic studies have assumed that rock uplift rates are an imposed and fixed property of the system [e.g., Howard *et al.*, 1994; Whipple *et al.*, 1999; Roe *et al.*, 2003]. In contrast, many geodynamical studies have often neglected the role of erosion [e.g., England *et al.*, 1985; Ellis *et al.*, 1995]. Relatively few geodynamic models have considered fully coupled interactions between tectonic deformation and surface erosion [e.g., Beaumont *et al.*, 1992, 2000]. Moreover the interpretation of

these numerical studies has been hampered by the absence of a theoretical framework capable of quantitative predictions.

[3] It is only recently that the burgeoning interest in tectonic geomorphology has brought these separate approaches together, combining climate, erosion, and tectonics into a single picture [Hilley *et al.*, 2004; Whipple and Meade, 2004, 2006; Roe *et al.*, 2006, 2008; Stolar *et al.*, 2006, 2007; Tomkin and Roe, 2007]. Of particular importance is the Coulomb wedge model, wherein the crust behaves as a Coulomb plastic material, and the orogen maintains a wedge-shaped, self-similar critical form during orogenesis [e.g., Chapple, 1978; Davis *et al.*, 1983; Dahlen, 1984, 1990]. The power of this approach is that it provides an essentially geometric rule for the role of tectonics in orogen evolution. This geometric rule can be combined with models of fluvial or glacial erosion to yield scaling relationships for the relative importance of the accretionary flux or the climate in setting the scale of the orogen and the rock uplift rates within it.

[4] The lessons learned from these conceptual models have been applied in a number of settings (e.g., the Olympics in Washington State [Stolar *et al.*, 2007], the European Alps [Willett *et al.*, 2006], the Pyrenees [Sinclair *et al.*, 2005], the Southern Alps of New Zealand [e.g., Tomkin and Roe, 2007], the St Elias range of Alaska, Taiwan [Whipple and Meade, 2006], Andes [Hilley *et al.*, 2004], and the Himalaya [Hilley and Strecker, 2004]). The concepts have proven useful in understanding interactions among climate, erosion and tectonics in these settings [see, e.g., Whipple, 2009].

<sup>1</sup>Department of Earth and Space Sciences, University of Washington, Seattle, Washington, USA.

<sup>2</sup>Department of Geology and Geophysics, Yale University, New Haven, Connecticut, USA.

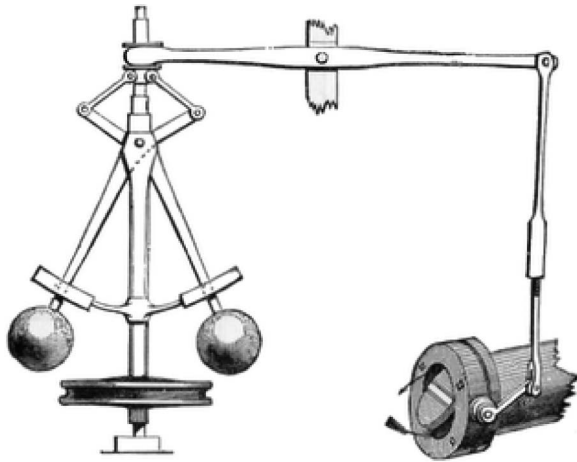


**Figure 1.** An example of a governor in an early steam engine [Routledge, 1900]. The outward or inward movement of the hinged balls, caused by faster or slower rotation of the belt-driven wheel on its axis, is linked mechanically to a valve on air intake of the steam engine and thus regulating, or governing, the speed of the engine.

[5] *Roe et al.* [2008] analyzed and quantified the tectonic and climatic feedbacks in this dynamical framework. They show that the self-similar form acts as a powerful “tectonic governor,” acting to damp the landscape response to changes climate and tectonic forcing. Mechanical governors came to the fore long ago during the development of the first practical engines that turned thermal energy into work. A governor (Figure 1) was needed to provide a feedback to regulate the process. *Maxwell* [1868] was first to mathematically describe the control that governor provided to the overall system. In many dynamical systems it is not only the individual processes, but the internal feedbacks that modulate how the system responds to changes. This recognition is central to understanding interactions in dynamic systems [Roe, 2009].

[6] Figure 2 depicts the operation of the tectonic governor in the setting of a small convergent orogen. As an example, envision a climate change that increases precipitation, which increases erosion rates and so tends to reduce orogen size. The tectonic requirement of self-similar form means the reduction in total relief (i.e., from toe to divide) is accompanied by a narrowing of the orogen. In turn, when a new equilibrium is attained, the narrower orogen means the same accretionary flux is focused into a smaller area, which enhances the local rock uplift rates and so opposes the original forcing. The system response is therefore damped, and so the mechanism is a negative feedback (or governor)

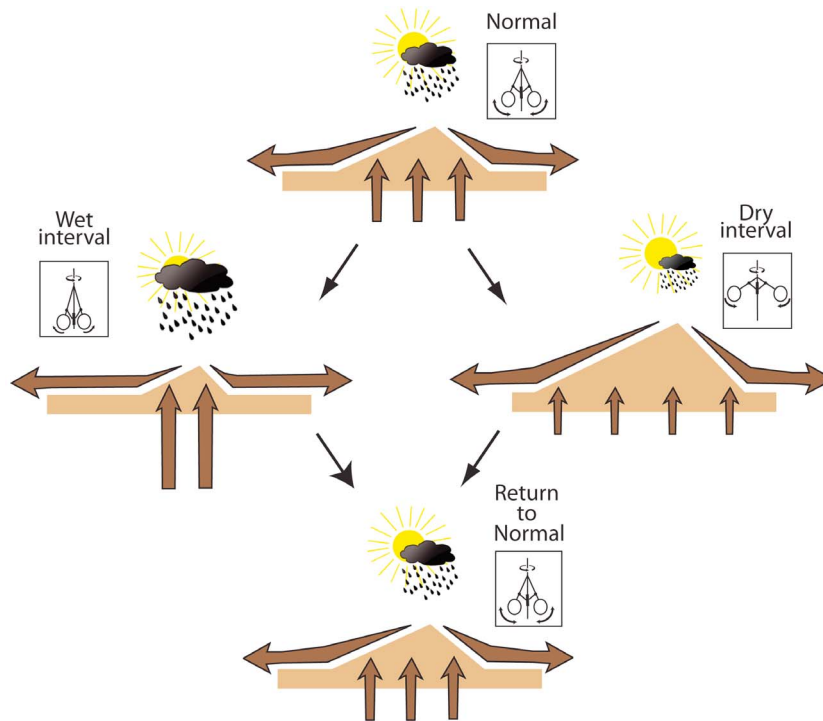


**Figure 2.** Schematic illustration of the tectonic governor. In equilibrium, the size of the orogen is governed by how big it must be for erosion yield to come into balance with the accretionary flux. To the extent that the orogen maintains a critical form, the orogen will shrink in both height and width in response to an interval of a climatically driven increase in erosion. Thus, rock uplift rates will be locally enhanced, creating a tendency opposing the erosional forcing. If the erosional forcing returns to its previous value and, again, if the orogen maintains a critical form, then the increase in rock uplift will act to restore the orogen to its previous size and shape. For a decrease in climatically driven erosion, the complementary argument also applies. The purpose is illustrative so it has been highly idealized; the general argument does not depend on the orogen root or on the material trajectories through the orogen.

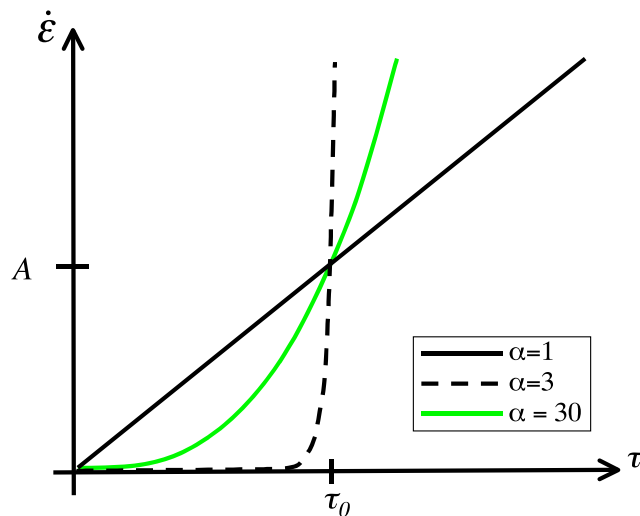


**Figure 3.** Illustration of different power law viscous rheologies from (13) for different values of the exponent  $\alpha$ .  $\tau_0$  is the normalizing stress at which the strain rate  $\dot{\epsilon} = A$ . As the value of  $\alpha$  approaches infinity, the material approaches plastic behavior. For a Coulomb plastic material,  $\tau_0$  increases linearly with depth within the material.

on topography. The key points are (1) that the Coulomb plastic rheology forces the orogen width and height to covary, and (2) that this covariation produces a negative feedback. The scaling relationships have been evaluated and confirmed in numerical models [Stolar *et al.*, 2006, 2007] and has been shown to be useful in understanding the relative strengths of tectonic and climatic feedbacks [Roe, 2009; Roe *et al.*, 2008].

[7] The preceding paragraphs summarize what is an almost total reversal of perspective: earlier geomorphological studies took the view that tectonics imposes the rock uplift rate, leaving erosion to set the form of the landscape; more recent studies would argue that it is tectonics that sets the form of the landscape (via the geometry it imposes), and that it is erosion rates that set the rock uplift rates (because they must balance at steady state).

[8] In this study, we explore how rheology affects the results arising from this new perspective. Davis *et al.* [1983] showed that the front region of many orogens have a taper consistent with a critical Coulomb wedge, and they also noted that wedges slopes tended to decrease rearward, as expected for the onset of thermal-activated viscous flow with the wedge interior.

[9] Our analysis is based on several assumptions. The first assumption is that the wedge is actively accreting, and that it receives enough precipitation to maintain an integrated fluvial drainage. Accretion and erosion are required to allow the wedge remain a steady state form.

[10] The second assumption is that the evolution and internal deformation of a convergent wedge can be represented as a continuum process. This assumption probably feels unnatural to anyone that has observed the complex array of faults and folds at the outcrop scale. Nonetheless, the continuum assumption has been applied with much success by many authors, starting with Elliott [1976], Chapple [1978] and subsequently by Cowan and Silling [1978], Davis *et al.* [1983], Dahlen [1990], and many others. Price [1973] pro-

vides a particularly nice articulation of this idea, noting that faults and folds are active at a local scale, but their contributions to deformation tend to become relatively smooth at the orogen scale. The same kind of analysis is used for dislocation glide in crystals. The deformation is discontinuous at the scale of atoms, but becomes relatively smooth and continuous at the scale of a mineral grain.

[11] The third assumption is that natural deformation can be represented with a single idealized rheological equation. The power law viscosity model has been widely used in geodynamic analysis because it covers a huge range of rheological behaviors with a just a few parameters [e.g., Chapple, 1969; Smith, 1975, 1977; England and McKenzie, 1982; Willett, 1999b]. A nice feature of the power law relationship is that it allows one to represent linear viscosity, as expected for pressure solution or diffusion-creep (where the stress exponent,  $\alpha \sim 1$ ), nonlinear viscosity as expected for dislocation-glide and climb in crystalline solids (where  $\alpha \sim 3$ ), and plastic behavior as expected for friction where the finite yield stress is simulated by a large stress exponent ( $\alpha \gg 3$ ). (We have to, somewhat inconveniently, use  $\alpha$  for the stress exponent rather than  $n$ , because  $n$  is also a conventional symbol in fluvial erosion laws.) We incorporate a depth dependence to this rheology, which allows us to consider the increase in yield stress that occurs with increasing depth for Coulomb plastics, and the decrease flow stress that occurs with depth due to the temperature-sensitive behavior of viscous materials. In summary, a continuum rheology cannot fully represent geologic structure, and should be interpreted as an “effective” rheology for the whole orogen.

[12] Our use of a power law rheology here is an efficient way of representing how tectonic accretion is distributed between changes in the thickness and width of the orogen. By varying just two parameters, we can span a large range of orogen-scale behaviors, from a highly nonlinear, Coulomb plastic orogen wherein width changes are proportional to height changes, through to a linear viscous orogen wherein the orogen spreads outward much more readily in response to height changes. Figure 3 illustrates the ability of the stress-exponent to represent a range of rheologies, from linear viscous, where  $\alpha = 1$ , to a more plastic behavior rheology, where  $\alpha$  is large and deformation rates start to become significant only after a stress threshold is reached. Using simple numerical integrations, we are also able to represent an orogen with a root that changes from nonlinear to linear behavior as the orogen changes size.

[13] We solve for the topographic form resulting from such a rheology. The lower the exponent on the power law rheology, the less sensitive the orogen height is to variations in orogen width. A striking result is that the topographic form is extremely insensitive to distributions of influx (accretion) or efflux (erosion) from a wedge. By insensitive, we mean that an orogenic wedge will tend to maintain a steady form, in the same sense as the critical taper concept, as originally proposed by Davis *et al.* [1983]. Our contribution is to extend this idea for the fully range of geologically applicable rheologies.

## 2. General Considerations

[14] We begin by identifying the basic conditions of the dynamical system that are necessary for specifying the

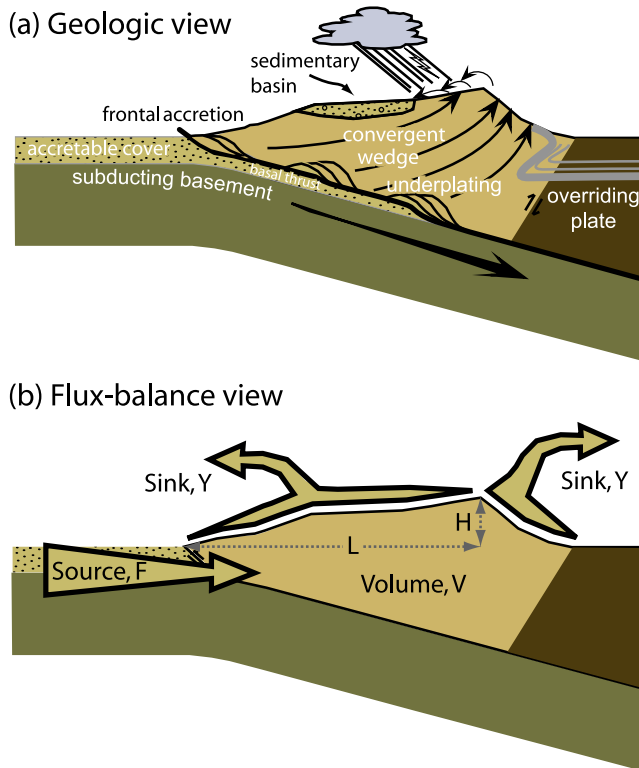


**Figure 4.** (a) Typical schematic illustration of various processes operating in orogenesis (note that the vertical is not to scale). (b) The same orogen dynamics distilled into a flux-balance problem. The flux balance dynamics are the basis of the scaling relationships derived in this study.

mutual interactions among climate, erosion, and tectonics. Figure 4a shows a geologic vision of processes affecting an orogenic wedge. Our view of the wedge is shown in Figure 4b, where the wedge is nothing more than a flux-balance problem, where the wedge is a volume that evolves based on balance between an accretionary influx and an erosion efflux. The relationship between the wedge volume and the wedge fluxes is governed by the critical topographic form of the orogen.

[15] The flux of material,  $F$ , incorporated into the wedge is ultimately driven by plate convergence. Let  $V$  be the volume of the wedge, and let its shape be loosely characterized in terms of its height,  $H$ , and width,  $L$ . Let  $Y$  be the total erosional yield from the orogen. Conservation of mass must apply,

$$\frac{dV}{dt} = F - Y. \quad (1)$$

In steady state, the accretionary flux equals the erosional yield [e.g., Brandon *et al.*, 1998; Whipple and Meade, 2006; Stolar *et al.*, 2006]. Recycling of eroded material is not considered here but could be incorporated without any loss of generality. The interactions between the three components of the system can be expressed in terms of three relationships (Figure 4b). First, the erosional yield is dependent on the climate and on the orogen shape, which can be written as

$$Y = Y(P, H, L). \quad (2)$$

Second, the shape of the orogen can be expressed as

$$H = H(L), \quad (3)$$

where the functional relationship is dependent mainly on rheology, and also on dip of the subducting plate. For an actively accreting Coulomb wedge, the wedge taper will always approach a critical taper angle dependent on the dip of the basal fault [Davis *et al.*, 1983]. The overall size of the wedge may change as the erosion changes, but the taper angle remains constant, so long as the basal dip remains constant. We show this concept of a critical topographic form also applies for all actively accreting wedges, regardless of their rheology, whether Coulomb plastic, linear viscous, or power law viscous.

[16] A relationship between climate and tectonics enters because of orographic precipitation [Roe *et al.*, 2008],

$$P = P(H, L). \quad (4)$$

Equations (1), (2), (3), and (4) are a complete set (i.e., both necessary and sufficient conditions) defining interactions among climate, erosion, and tectonics. In the broadest terms, orogen dynamics can be conceptualized as a classic flux-balance problem (Figure 4b), with a source,  $F$ , a sink,  $Y$ , and a reservoir,  $V$ . However in contrast to a simple “bucket-style” flux reservoir, an orogenic wedge has a more complex dependence on the interactions with accretionary fluxes, orographic precipitation, and rheology. Our focus here is on how rheology affects equilibrium scaling relationships for an actively accreting wedge. The steady state case provides the essential basis for understanding the timescale for transient behavior [Whipple and Meade, 2006; Stolar *et al.*, 2006; Roe *et al.*, 2008].

### 3. Orogen-Width Scaling Relationship

[17] We consider a system dominated by fluvial erosion, and follow essentially the same procedure as Whipple and Meade [2004] and Roe *et al.* [2006], using the notation of the latter. We focus here on a one-sided wedge, because Whipple and Meade [2004] and Roe *et al.* [2008] show that a two-sided wedge obeys the same scaling relationship. The fluvial-erosion rate follows a standard formulation [e.g., Howard, 1980; Whipple, 2004],

$$\dot{e} = KQ^m \left( \frac{dz}{dx} \right)^n, \quad (5)$$

where  $Q$  is the discharge and  $dz/dx$  is the along-channel slope of the river. Precipitation,  $P$ , is assumed uniform. Stolar *et al.* [2007] have shown that, for realistic precipitation rates, orogen size and deformation pattern are relatively insensitive to the pattern of precipitation. Using Hack’s law for the relationship between channel length and drainage area [Hack, 1957], we can write

$$Q = Pk_a x^h. \quad (6)$$

$K$ ,  $k_a$ ,  $h$ ,  $m$ , and  $n$  are constants reflecting the rock erodibility, the drainage network structure, and the dominant physical process governing fluvial erosion.



[18] In steady state, the local rock uplift rate,  $U$ , balances the local erosion rate. Hence, we can write

$$U = Kk_a^m P^m x^{hm} \left( \frac{dz}{dx} \right)^n. \quad (7)$$

Assuming uniform rock uplift, (7) can be integrated from the toe of the orogen to a point near the divide,  $(x_c, z_c)$ , where the discharge is so low that fluvial erosion no longer applies and hillslope processes (i.e., landslides, soil creep, etc.) take over as the dominant mechanism of erosion. The difference in elevation from the toe of the wedge to the highest point of fluvial erosion is called the fluvial relief,

$$z_c = \frac{1}{(1 - hm/n)} \left( \frac{U}{Kk_a^m P^m} \right)^{\frac{1}{n}} \left[ L^{1 - \frac{hm}{n}} - x_c^{1 - \frac{hm}{n}} \right]. \quad (8)$$

There is a special case, where  $hm/n = 1$  [e.g., *Whipple et al.*, 1999; *Roe et al.*, 2006], but the scaling relationship derived below applies to this case as well. It must, since the scaling relationship has to vary smoothly with small changes in model parameters, and the limiting case of  $hm/n \rightarrow 1$  can be approached from either side.

[19] We refer readers to earlier papers [e.g., *Hilley et al.*, 2004; *Whipple and Meade*, 2004; *Roe et al.*, 2006] for details of the derivation, but a sketch of the solution is provided here. First, in fluvially eroding orogens, the fluvial relief comprises the greater part of the total relief,  $H$ , defined as the maximum elevation of the drainage divide above the foreland. Hence  $z_c \approx H$ . Second, the distance from channel head to the drainage divide is also typically small compared to the channel length, and so  $x_c \ll L$ . Finally, if rock uplift is uniform, it is related to the accretionary flux,  $F$ , by:  $U = F/L$ . Substituting these three conditions into (8) and rearranging gives the following proportionality,

$$H^n \propto \left( \frac{F}{LP^m} \right) L^{n-hm}. \quad (9)$$

For an fluvially eroded orogen, this expression governs the relationship between  $H$ ,  $L$ ,  $P$ , and  $F$  in steady state.

[20] Several results derived by *Roe et al.* [2006] show this relationship is largely independent on the underlying assumptions. The exponents in the scaling relationship are insensitive to how the channel is connected to the drainage divide. Furthermore, the rock uplift can depart significantly from uniform, provided that it scales in an approximately self-similar manner with orogen size. These conclusions are supported by the numerical modeling and theoretical results of *Stolar et al.* [2006, 2007].

[21] The final step in deriving the orogen-width scaling relationship is to include how the deformation within the orogen controls the topographic form, or in other words, how it controls the relationship between  $H$  and  $L$ . In the next section, it is shown that a power law viscous rheology produces a relationship of the form,

$$H \propto L^\psi. \quad (10)$$

Substituting this into (9), gives

$$F \propto P^m L^{1+hm} L^{n(\psi-1)}. \quad (11)$$

This equation is a general expression for the balance between  $F$ ,  $L$ , and  $P$ . It holds provided that the height of the orogen can be expressed as a power law function of  $L$ .

[22] A critical Coulomb wedge with a constant basal dip has a constant taper angle, and so  $H \propto L$  and  $\psi = 1$ . Therefore,

$$L \propto F^{\frac{1}{1+hm}} P^{\frac{-m}{1+hm}}. \quad (12)$$

This is the relationship derived by *Roe et al.* [2006] and is essentially the same as in the works of *Hilley et al.* [2004] and *Whipple and Meade* [2004]. We set  $h = 2$  [e.g., *Hack*, 1957; *Montgomery and Dietrich*, 1992], and consider three different combinations of  $(m, n)$ : (1/3, 2/3), (1/2, 1), and (1, 2). The exponents on  $F$  and  $P$  in (12) are (3/5, -1/5), (1/2, -1/4), and (1/3, -1/3), respectively [*Roe et al.*, 2006]. The low values of these exponents imply that the orogen width is insensitive to changes in precipitation rate and accretionary flux.

## 4. Topographic Form and Power Law Rheologies

### 4.1. Defining a Power Law Rheology

[23] Tectonic deformation can be envisioned to be driven by far-field tectonic stresses, operating subparallel to the horizontal, and to body forces related to the topography. The rheology of the crust relates the stresses and strain associated with these loadings. As used here a linear viscous rheology and a nonlinear ‘‘power law’’ rheology indicate different sensitivities of strain rate to stress (Figure 3). A linear or Newtonian viscosity exhibits a simple proportionality between stress and strain rate. A power law rheology has a greater ‘‘sensitivity’’ to increasing stress, given that the strain rate is proportional to the deviatoric stress raised to a exponent greater than 1. Dislocation glide-and-climb is the typical viscous mechanism in the crust, and it has a stress exponent  $\approx 3$ . Viscous materials will flow at any deviatoric stress, although the strain rates may be quite small. In contrast, plastic materials have a finite yield strength, so strain rates will remain at zero until the yield stress is exceeded. Frictional materials have this property, in that deformation does not occur until reaching a critical yield stress. Frictional materials are distinguished from other plastic materials in that the yield stress for frictional materials is a function of pressure, a feature that is indicated by the term Coulomb plastic. Coulomb plastic materials become stronger with depth, given that mean stress or pressure increases with depth (ignoring pore fluid pressures for the moment). Viscous rheologies generally become weaker with depth because these rheologies are sensitive to temperature. In this sense, both rheologies have a depth sensitivity, but they are distinguished by opposing sensitivities. It is possible to write a general expression for the rheology that encompass all of these possibilities in terms of two free parameters. First, let

$$\dot{\epsilon} = A(\tau/\tau_0)^\alpha, \quad (13)$$

where  $\dot{\epsilon}$  is the strain rate and  $\tau$  is the deviatoric stress, which follows Norton’s law for steady state creep in engineering [*Norton*, 1929] and Glen’s law in glaciology [*Glen*, 1955].  $A$  is a flow factor which we initially assume constant. In

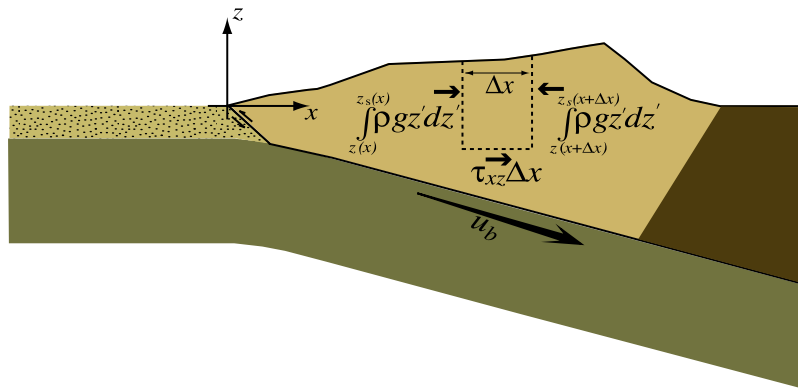


**Figure 5.** Illustration of the horizontal forces acting on an element within the wedge, shown by the dashed line. The pressure gradient force integrated along the vertical sides of the element is balanced by the shear stress along the bottom face of the element. Within this model framework, the longitudinal deviatoric stress components are negligible because the depth scales are assumed to be much smaller than horizontal scales within the wedge [e.g., *Emerman and Turcotte, 1983*].

general,  $A$  might also contain some temperature dependence reflecting that the hotter the crust is, the more easily it tends to deform [e.g., *England, 1983; Stüwe, 2002*]. We explore the effect of such a dependence in section 7.  $\alpha$  determines the nonlinearity of the stress - strain rate relationship: if  $\alpha = 1$ , the fluid is linear; if  $\alpha = \infty$  the fluid is plastic (see Figure 3).

[24] Second, we define  $\tau_0$  as a normalizing stress, given by

$$\tau_0 = \tau^* \left( \frac{z_s - z}{D_0} \right)^\beta, \quad (14)$$

$\tau^*$  and  $D_0$  are constants,  $(z_s - z)$  is the depth below the surface,  $z_s$ , and  $\beta$  is the exponent governing the depth dependence of  $\tau_0$ . The power law depth variation of  $\tau_0$  is used here for mathematical convenience, and is not intended to represent any real process. Consider the case of  $\alpha = \infty$ : if  $\beta = 0$ , the threshold stress is constant and the material is perfect plastic; if  $\beta = 1$ , the material is Coulomb plastic. Note that we ignore the cohesion term for Coulomb friction given that this term becomes insignificant for wedges that are thicker than about 5 km [*Dahlen, 1990*]. Thermal-activated viscosity could be represented by  $\beta < 0$ .

[25] The power law rheology in (13) and (14) is a generalized representation that is able to mimic a wide range of orogen behaviors. By selecting different values of  $\alpha$  and  $\beta$ , this behavior runs the gamut from a “stiff,” Coulomb plastic material, in which height and width changes are proportional to each other, through to a more fluid viscous material in which the wedge spreads out far in response to small changes in size. These rheologies represent continuum-scale approximations and are appropriate for studying the overall evolution of the wedge. They should not be taken as representative of discontinuous and heterogeneous processes, such as faults, folds, and other structures, which are the most visible aspect of orogenic deformation at the subcontinuum scale. Physical models like sandbox experiments that do have localized deformation and discrete faults do also show that the large-scale behavior of the full pile of sand can be interpreted in terms of wedge dynamics, and characterized

by the relationship between its height and its width [e.g., *Davis et al., 1983; Hoth et al., 2006*].

## 4.2. Topographic Form

[26] Our generalized power law rheology in (13) and (14) can be used to solve for the topographic form of an orogen governed by such a rheology. In section 5, this topographic form will be combined with (11) to obtain a scaling relationship between accretionary flux, precipitation rate, and orogen width. We follow the scale analyses and approximations of *Emerman and Turcotte [1983]*, who invoked the equations of lubrication theory to derive their results. We extend their analyses to include the depth dependency of typical geologic rheologies. The method of solution also ends up being similar to that for glaciers and ice sheets using the shallow-ice approximation [e.g., *Hutter, 1983; Paterson, 1994*]. The solution provides an efficient way of sampling a wide range of height-width relationships for wedges.

[27] The main assumption that simplifies the solution is that the characteristic horizontal length scales are much larger than characteristic depth scales, or in other words, the aspect ratio of the orogen is large. *Emerman and Turcotte [1983]* show this implies that horizontal gradients in shear stress are negligible compared to those in the vertical. This is a different physical model from the thin sheet approximation appropriate for plateaux or systems with weak detachment [e.g., *England and McKenzie, 1982*], where the strain rates are vertically averaged and the force balance is between the pressure gradient due to the topography, the longitudinal stresses and, possibly, some stipulated basal traction [e.g., *Ellis et al., 1995*]. *Batchelor [2000]* and *Pollard and Fletcher [2005]* review how this “lubrication theory” assumption applies to typical geodynamic problems.

[28] A schematic illustration of the forces acting on an element within the orogen is shown in Figure 5. The assumptions of a large aspect ratio and of zero stress on the upper surface mean the fundamental force balance reduces to the shear stress on the lower face of the element,  $\tau_{xz}$ , and the integral of the pressure gradient acting on the vertical sides of the element. Let  $x$ ,  $z$  and  $u$ ,  $w$  be the horizontal and

vertical coordinates and rock velocities, respectively. The force balance can be expressed as

$$\tau_{xz} = \rho_c g (z_s - z) \frac{dz_s}{dx}, \quad (15)$$

where  $\rho_c$  is the density of the crust,  $g$  is the gravitational constant, and  $z_s$  is the surface elevation. The large aspect ratio also means that the total strain rate is dominated by the vertical gradient in the horizontal velocity. Substituting into (13),

$$\frac{du}{dz} = A \left( \frac{\tau_{xz}}{\tau_0} \right)^\alpha. \quad (16)$$

The boundary conditions are that the rock velocity is specified ( $u_b$ ,  $w_b$ ) at the base of the orogen,  $z = z_b$ , and that the erosion rate at the surface of the orogen is  $\dot{e}$ . Although it is not necessary for the functional form of the topographic profile, we can also consider a local isostatic balance, which relates  $z_s$ ,  $z_b$ , and the total thickness of the orogen,  $h_T$ ,

$$\begin{aligned} z_s &= \left(1 - \frac{\rho_c}{\rho_m}\right) h_T \\ z_b &= -\left(\frac{\rho_c}{\rho_m}\right) h_T, \end{aligned} \quad (17)$$

where  $\rho_m$  is the density of the underlying mantle. Isostasy is important in deriving the time-dependent behavior of the system, since it affects the amount of material needed to build an orogen of a given size [Whipple and Meade, 2006; Stolar *et al.*, 2006].

[29] In this two dimensional framework, the horizontal flux of rock,  $F$ , past any given point is given by the integral of the horizontal velocity,

$$F(x) = \int_{z_b}^{z_s} u(x, z) dz, \quad (18)$$

Using equations (14), (15), and (17), (16) can be integrated twice in the vertical, subject to the boundary conditions, to give

$$F(x) = u_b h_T - \left\{ \frac{A(\rho_c g)^\alpha D_0^{\alpha\beta} (1 - \rho_c/\rho_m)^\alpha}{\tau^{*\alpha}} \right\} \cdot h_T^{\alpha(1-\beta)+2} \left( \frac{dh_T}{dx} \right)^\alpha. \quad (19)$$

The horizontal flux of material within the orogen can thus be thought of as having two components: a translational component due to drag in the lower part of wedge by the subducting plate, represented by the first RH term in (19), and a deformation component in the opposite direction, due to the viscous rheology and given by the second RH term in (19).

[30] Another constraint is conservation of mass, which requires at each point,

$$\frac{\partial h_T}{\partial t} = w_b - \dot{e} - \frac{\partial F}{\partial x}, \quad (20)$$

where  $w_b - \dot{e}$  (i.e., underplating minus erosion) can be thought of as the net mass balance at a given point. In steady state,  $\partial h_T / \partial t = 0$ , and so

$$F(x) = \int_0^x (w_b - \dot{e}) dx. \quad (21)$$

For a one-sided wedge, the mass balance integrated from any given point to the orogen divide is balanced by the flow, or deformation, of rock within the orogen at that point. From (17) and (19),  $F$  can be expressed in terms of  $h_T$  and its first derivative, and so as recognized by *Emerman and Turcotte* [1983], (21) is essentially a nonlinear diffusion equation that can be solved for the profile  $h_T(x)$ .

[31] A second important assumption made by *Emerman and Turcotte* [1983] is that the thickness of the crustal layer being accreted into the wedge,  $\delta$ , is much less than the total thickness of the wedge,  $h$  (i.e., including the crustal root). Crucially, *Emerman and Turcotte* demonstrated that the integral on the right-hand side of (21) can be neglected when solving for the profile of the wedge. The integral scales as  $w_b L$ , which is the rock uplift integrated over the width of the orogen. Conservation of mass means that this quantity must equal the accretionary flux, or  $u_b \delta$ . Since  $\delta \ll h$ , the integral is much less than the first term on the right-hand side of (19). Therefore, the steady state solution for the wedge profile (20) boils down to solving  $F = 0$ . Using (17) and (19), we get

$$u_b h_T - A' \cdot h_T^{\alpha(1-\beta)+2} \left( \frac{dh_T}{dx} \right)^\alpha, \quad (22)$$

where all of the constants have been subsumed into  $A'$ .

[32] It seems counterintuitive to solve for  $F = 0$  when the orogen depends on a mass flux for its existence, and we emphasize that this approximation is only valid in calculating the shape of the wedge profile, and cannot be used in calculating the size of the orogen [*Emerman and Turcotte*, 1983]. The solution to (22) can be regarded as a ‘‘critical’’ topographic form, the profile that the orogen will attain for the particular rheology governing its deformation.

[33] Using (17), (22) can be rearranged and expressed as a first-order differential equation for  $h_T$ . Integrating from  $x = 0$  to  $L$ , assuming  $h_T = 0$  at  $x = L$ , gives

$$h_T(x) = A'' (L - x)^{\frac{\alpha}{\alpha(2-\beta)+1}}, \quad (23)$$

where  $A''$  is a constant. (For specified patterns of  $u_b$ , velocities within the wedge can be found by integrating (16). *Emerman and Turcotte* [1983] solve for the return flow at the surface of the wedge, assuming no frontal accretion or erosion. For the rheology used here, this velocity is given by  $u = u_b / (\alpha(1 - \beta) + 1)$ , predicting some surface extension, even as the limit of a Coulomb plastic rheology is approached [e.g., *Buck and Sokoutis*, 1994; *Willett*, 1999b].)

[34]  $H$  is the maximum height of the orogen (i.e.,  $H = z_s(0)$ ), and so in isostatic equilibrium it scales in the same way as  $h_T(0)$  (see (17)). Hence from (23),

$$H \propto L^{\frac{\alpha}{\alpha(2-\beta)+1}}. \quad (24)$$

For a linear viscous rheology with no temperature dependence  $\alpha = 1$  and  $\beta = 0$ , giving  $H \propto L^{\frac{1}{3}}$ , as found by *Emerman and Turcotte* [1983]. For a typical nonlinear viscosity with no temperature dependence,  $\alpha \sim 3$  and  $\beta = 0$ , giving  $H \propto L^{\frac{3}{7}}$ . For viscous rheologies, the decrease in viscosity with temperature and depth means that these estimates are upper bounds. In the case of a Coulomb plastic rheology,  $\alpha = \infty$  and

**Table 1.** Exponents on the Orogen-Width Scaling Relationship:  $L \propto F^{\gamma_1} P^{\gamma_2}$ <sup>a</sup>

m	n	h	Coulomb Plastic ( $\psi = 1$ )		Linear Viscous ( $\psi = \frac{1}{3}$ )	
			$F^{\gamma_1}$	$P^{\gamma_2}$	$F^{\gamma_1}$	$P^{\gamma_2}$
$\frac{1}{3}$	$\frac{2}{3}$	2	$\frac{3}{5}$	$-\frac{1}{5}$	$\frac{9}{11}$	$-\frac{3}{11}$
$\frac{1}{2}$	1	2	$\frac{1}{2}$	$-\frac{1}{4}$	$\frac{3}{4}$	$-\frac{3}{8}$
1	2	2	$\frac{1}{3}$	$-\frac{1}{3}$	$\frac{3}{5}$	$-\frac{1}{3}$

<sup>a</sup>Table 1 shows a comparison for two different rheologies (Coulomb plastic and linear viscous) and for three different commonly assumed erosion processes. The exponents are a measure of the sensitivity of the orogen width to changes in  $F$  and  $P$ . A linear viscous rheology makes orogen width more sensitive to change in  $F$  and  $P$ , but not dramatically so. See text for more details.

$\beta = 1$ , and so  $H \propto L$ . Thus, the analysis reproduces the critical taper angle of a Coulomb critical wedge.

## 5. Orogen Scaling-Relationships for a General Rheology

[35] Having obtained the solution for the topographic form for a general rheology, it can now be used to calculate how the orogen-width scaling relationship is influenced by rheology. From (24), the expression for  $\psi$  in (11) is given by

$$\psi = \frac{\alpha}{\alpha(2 - \beta) + 1}. \quad (25)$$

Equation (11) can be rearranged to express  $L$  as a function of  $F$  and  $P$ ,

$$L \propto F^{\gamma_1} P^{\gamma_2}. \quad (26)$$

where  $\gamma_1$  and  $\gamma_2$  are functions of  $h$ ,  $m$ ,  $n$ , and  $\psi$ . Table 1 presents these exponents for Coulomb plastic and linear viscous rheologies, and for the three different sets of commonly assumed fluvial erosional parameters. In agreement with previous studies,  $\gamma_1$  is greater than or equal to  $\gamma_2$ , meaning that for most parameter combinations, the orogen width is more sensitive to changes in tectonic forcing than to changes in climate. Further,  $\gamma_1$  and  $\gamma_2$  are both less than one, reflecting the strong negative feedback of the tectonic governor, as explained in more detail in sections 5.2 and 5.3. The values of  $\gamma_1$  and  $\gamma_2$  are larger for the linear viscous rheology than for the Coulomb plastic rheology. This reflects the fact that a linear viscous orogen spreads out more for a given change in volume than a Coulomb plastic orogen.

[36] A striking result is that, even though the two end-member rheologies are very different, the rheology has little influence on the exponents in the orogen-width scaling relationship. In other words, the impact of precipitation and tectonic forcing on the width of an orogen is quite insensitive to the specific rheology governing the deformation. The reason can be seen by comparing the two exponents on  $L$  on the right-hand side of (11). The first exponent,  $1 + hm$ , reflects two factors: (1) the  $hm$  comes from the dependence of fluvial erosion on discharge and also the fact that upstream drainage area accumulates with downstream distance; and (2) the 1 comes from the fact that the local erosion rates must be integrated over the whole orogen

width to balance the total incoming accretionary flux. The effect of rheology on the topographic form is folded into the second exponent,  $n(\psi - 1)$ . For the range of rheologies considered here  $1/3 \leq \psi \leq 1$ . The effect of rheology is thus biggest for smaller values of  $\psi$ . For a linear viscous rheology with  $\psi = 1/3$  and the three different combinations of erosion parameters, the relative sizes of the first and second exponents on  $L$  in (11) are 15:4, 3:1, and 9:4. Thus, orogen width is much more sensitive to discharge and drainage area than to rheology.

### 5.1. Other Orogen Attributes

[37] In addition to its width, the model orogen can be characterized by two other attributes: height and rock uplift. These attributes are related to the orogen width via the rheology, which gives the topographic form  $H \propto L^\psi$ , and via the conservation of mass, which requires  $U = F/L$ . Therefore, the dependence of  $H$  and  $U$  on the forcing variables  $F$  and  $P$  can also be expressed in terms of scaling relationships.

[38] Table 2 gives the exponents on these scaling relationships for the case of  $(h, m, n) = (2, 1/2, 1)$ , and illustrates the behavior of these attributes for different rheologies. For completeness, we also include the cases of a fixed-width orogen and a plateau (which can be emulated by setting  $\psi = \infty$  and  $\psi = 0$ , respectively, in (10)). As  $\psi$  decreases, the orogen width becomes more sensitive to changes in  $F$  and  $P$ . At the same time, the height becomes less sensitive to these forcings since it becomes harder to build high topography. Also, as the width becomes more sensitive to accretionary forcing, the rock uplift rate becomes less sensitive: a large increase in width means the accretionary flux is distributed over a larger area, damping the change in the rock uplift rates.

### 5.2. Why Does an Orogen Change so Little in Response to Changes in Forcing?

[39] For all of the rheologies considered, the orogen response to changes in climate and tectonic forcing is small. All of the exponents in Table 2 are less than or equal to one. These exponents can also be interpreted as the factor multiplying the fractional response of that orogen attribute to a fractional change in the forcing. For example, from Table 2, the fractional change in rock uplift rate for a linear viscous wedge is given by

$$\frac{\Delta U}{U} = \frac{1}{4} \frac{\Delta F}{F} + \frac{3}{8} \frac{\Delta P}{P}. \quad (27)$$

Thus, to bring about dramatic changes in orogen attributes (an order of magnitude, say), extremely large fractional changes

**Table 2.** Exponents on Scaling Relationships for Different Orogen Attributes: Width, Height, and Rock Uplift<sup>a</sup>

	Width, $L$		Height, $H$		Rock Uplift, $U$	
	$F^{\gamma_1}$	$P^{\gamma_2}$	$F^{\gamma_1}$	$P^{\gamma_2}$	$F^{\gamma_1}$	$P^{\gamma_2}$
Fixed width ( $\psi = \infty$ )	0	0	1	$-\frac{1}{2}$	1	0
Coulomb plastic ( $\psi = 1$ )	$\frac{1}{2}$	$-\frac{1}{4}$	$\frac{1}{2}$	$-\frac{1}{4}$	$\frac{1}{2}$	$\frac{1}{4}$
Linear viscous ( $\psi = \frac{1}{3}$ )	$\frac{3}{4}$	$-\frac{3}{8}$	$\frac{1}{4}$	$\frac{1}{8}$	$\frac{1}{4}$	$\frac{3}{8}$
Plateau ( $\psi = 0$ )	1	$-\frac{1}{2}$	0	0	0	$\frac{1}{2}$

<sup>a</sup>Here  $(h, m, n) = (2, 1/2, 1)$  was assumed for the values shown. The case of a plateau is included for completeness, but as noted in the text, the results derived for this case should be interpreted cautiously.



**Table 3.** Feedback Factors and Corresponding Gains for Width, Height, and Rock Uplift Rates for Different Rheologies<sup>a</sup>

	$f_L$	$f_H, f_U$	$G_L$ (%)	$G_H, G_U$ (%)
Fixed width ( $\psi = \infty$ )	$-\infty$	$\frac{1}{2}$	0	200
Coulomb plastic ( $\psi = 1$ )	0	0	100	100
Linear viscous ( $\psi = \frac{1}{3}$ )	$\frac{1}{3}$	-1	150	50
Plateau ( $\psi = 0$ )	$\frac{1}{2}$	$-\infty$	200	0

<sup>a</sup>The Coulomb plastic rheology is taken as the reference case, and the expressions for the feedback factors are derived in Appendix A.  $(h, m, n) = (2, 1/2, 1)$  was assumed for the values shown. Because  $hm/n = 1$ ,  $f_H = f_U$ , but this is not generally true. The gains are given as percentages and are related to the fractional feedback factors by  $G = 1/(1 - f)$ . When multiple feedbacks are present, feedback factors add linearly, whereas gains do not. The case of a plateau is included for completeness; the results should be interpreted cautiously.

in the forcing factors are required. This reflects the strong damping tendency of the tectonic governor. Recalling from (1) that, in equilibrium  $F = Y$ , equation (11) shows that erosional yield is a sensitive function of orogen width. Fundamentally this is a consequence of Hack's law. For example, an increase in the orogen width increases the drainage area of the river network. The erosional yield (and thus the sink of mass from the system) increases dramatically, and so provides a powerful opposing tendency to the increasing width.

[40] Although changes in forcing are obviously hard to estimate over geologic time, some factors like average precipitation rates can be partly constrained on physical grounds. For example, all else being equal, the moisture-carrying capacity of the atmosphere limits the precipitation rate. A useful rule of thumb is that an increase of 10°C doubles the moisture content of the air, and an increase of 30°C, increases moisture content by an order of magnitude [e.g., Roe, 2005]. Both correspond to enormous climate changes that might have independent observable evidence. So in evaluating scenarios put forward to explain particular orogen histories, the exponents in Table 2 might be used to assess their physical plausibility.

### 5.3. Feedback Analysis

[41] An alternative way to characterize the strength of interactions in a system is through a feedback analysis. Roe *et al.* [2008] used a model of orographic precipitation to analyze of the strength of precipitation feedback for a critical Coulomb plastic wedge. We use the same procedure to characterize how changing the governing rheology affects the sensitivity of the orogen properties to the magnitude of the accretionary flux and the precipitation rate.

[42] A formal feedback analysis includes defining gains and feedback factors, which are essential in comparing the strength of different interactions in a system [e.g., Roe, 2009]. Roe *et al.* [2008] only considered a Coulomb plastic critical wedge, and used a fixed-width wedge as a reference, no feedback, case. To consider the role of rheology in this feedback analysis, we define the Coulomb critical wedge as the reference case. Thus the feedback factors and gains discussed here provide quantitative predictions about how the wedge will change relative to a Coulomb critical wedge. Secondly, this reference case also allows for a direct comparison with the detailed analysis of the precipitation feedback in Roe *et al.* [2008], which also took the Coulomb critical wedge as the reference case.

[43] Let  $\Delta L_0$  be the change in orogen width for an increment in accretionary forcing  $\Delta F_0$  in the reference case. Now let  $\Delta L$  be the width change to that same increment in accretionary forcing, but with a different rheology (i.e., non-Coulomb plastic). The feedback factor,  $f_L$ , and gain,  $G_L$ , relate these two length changes,

$$\Delta L = G_L \Delta L_0 = \frac{\Delta L_0}{1 - f_L}. \quad (28)$$

One might wonder why it is necessary to define both gains and feedback factors given that  $G_L = (1 - f_L)^{-1}$ . The gains provide the most direct representation of the feedback, but the feedback factors have the advantage in that they are linearly additive, so one can easily compare different feedback mechanisms or combine these feedback factors to see how they might active together. As a consequence, both variables are important to understanding feedbacks in a dynamic system [e.g., Roe, 2009].

[44] In Appendix A, expressions for the feedbacks factors are derived for the orogen width,  $f_L$ , the orogen height,  $f_H$ , and the rock uplift rate,  $f_U$ . They are

$$\begin{aligned} f_L &= \frac{n(1-\psi)}{1+hm}, \\ f_H &= \frac{(\psi-1)(1+hm-n)}{\psi(1+hm)}, \\ f_U &= \frac{n(\psi-1)}{(1+hm)[hm-n(1-\psi)]}. \end{aligned} \quad (29)$$

The calculations for  $(h, m, n) = (2, 1/2, 1)$  are presented in Table 3. Because of the choice of  $hm/n = 1$ ,  $f_H = f_U$ , although this is not always true and in general the feedback factors can be quite different from each other. Consider the change in feedbacks as one replaces the reference case, with a Coulomb plastic rheology represented by  $\psi = 1$ , to a more viscous rheology as defined by decreasing values of  $\psi$ . A lower  $\psi$  value causes an increased sensitivity of orogen width to changes in accretionary forcing. In contrast, the sensitivity of orogen height and rock uplift rates decreases with decreasing  $\psi$  values. In the limiting case of a plateau, there is no change in orogen height and only outward growth of the wedge.

[45] Roe *et al.* [2008] found that large precipitation feedbacks were possible if only the leeward (i.e., rain shadow) flank of the orogen were considered. However, these feedbacks were strongly muted when both flanks of the orogen were coupled together. For two-sided wedges, Roe *et al.* [2008] found that, under typical choices of model parameters, the width feedback factor,  $f_L$ , for a precipitation feedback varies from between approximately -0.4 and +0.2. Feedback factors are directly comparable, and so from Table 3, it can be seen that changing the rheology from Coulomb plastic to linear viscous has about the same effect as adding orographic precipitation.

## 6. Effect of Mass Balance Patterns

[46] In deriving the solution for the topographic form in section 4.2, scaling arguments are used to argue that the mass balance,  $w_b - \dot{e}$  (i.e., the underplating minus the erosion rate), could be neglected. In this section, we explore the validity of this approximation using a numerical solution of (21).

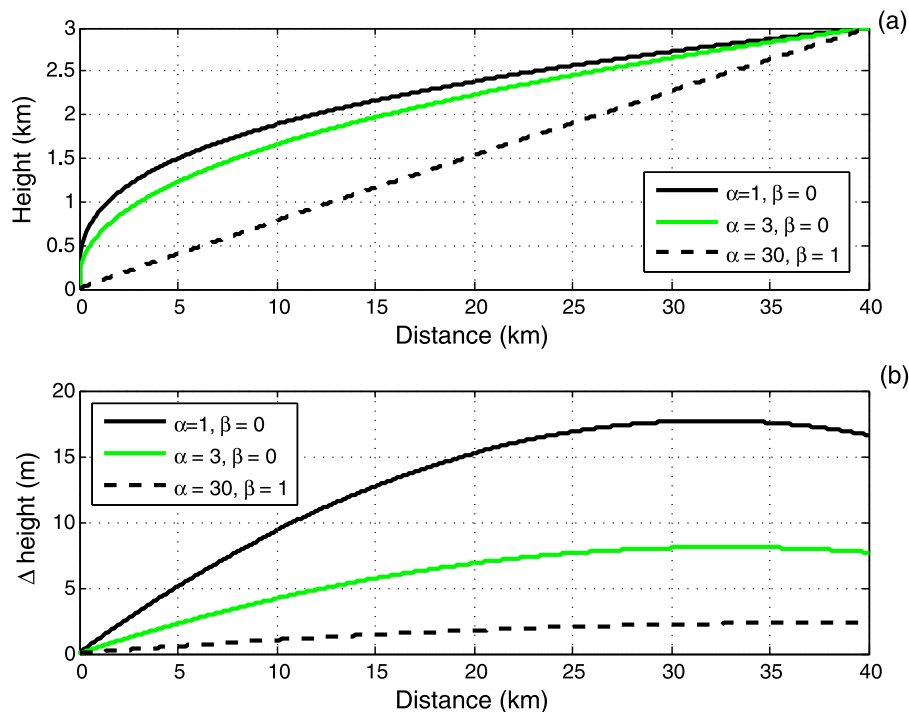


**Figure 6.** For different rheologies, (a) critical form profiles for the mass balance pattern in (30) using the positive sign and (b) the change in profile elevation when the sign of mass balance pattern is reversed. Note the change of  $y$  axis scale between Figures 6a and 6b. Figure 6 shows that the critical form of the orogen is extremely insensitive to the assumed pattern of the mass balance, with rheologies that are near Coulomb plastic being the least sensitive.

[47] As noted in section 4.2, the typical magnitude of the mass balance can be constrained from mass continuity:  $w_b$  and  $\dot{\epsilon}$  scale as  $u_b\delta/L$ . However, the pattern of the local mass balance is, as yet only loosely constrained from observations or theory [e.g., *Willett*, 1999b, 2001; *Stolar et al.*, 2007]. Despite these uncertainties, we can approximate how different distributions of erosion rates might affect the feedback sensitivities of the wedge. To do this, we define two simple end-member cases for the distribution of the local mass balance,

$$w_b - \dot{\epsilon} = \pm \frac{u_b\delta}{L} \left( \frac{x}{L} - \frac{1}{2} \right). \quad (30)$$

The erosion rate varies linearly across the wedge, with the fastest erosion at the rear of the wedge for the positive sign, and at the front of the wedge for the negative sign. This functional form ensures a flux balance, and therefore a steady state solution for a given  $L$ . Note that locally  $w_b - \dot{\epsilon}$  is not zero, and so at steady state, it must be balanced by the divergence or convergence of the vertically integrated horizontal flux within the orogen.

[48] We consider an orogen with the following scales  $L = 40$  km,  $\delta = 5$  km,  $u_b = 16$  mm yr<sup>-1</sup>, giving an average uplift rate of 2 mm yr<sup>-1</sup>. Crustal and mantle densities are assumed to be  $2.8 \times 10^3$  and  $3.3 \times 10^3$  kg m<sup>-3</sup>, respectively. Since we only consider values of 0 or 1 for  $\beta$ , the value of  $D_0$  in (19) is arbitrary except for how it influences the other parameters, but we take it to be 30 km. The ratio of  $A/\tau^*$  is then chosen to give a realistic  $H = 3$  km for the standard case.

[49] At the toe of the wedge,  $u_b h$  is finite and the thickness is zero. From (19), if  $\alpha$  is finite then  $dz_s/dx$  must go infinity there, and this causes difficulty in achieving numerical convergence. Appendix B gives a horizontal coordinate transformation that was used to ensure that, in the new coordinate frame, the slope at the toe remains finite. A standard numerical ODE-solver was then used to solve the transformed (19). After converting back to the original  $x$  coordinate, the result is the topographic form for a given rheology and mass balance pattern.

[50] We consider three different combinations of the rheology parameters  $\alpha$  and  $\beta$ : a linear viscous case,  $(\alpha, \beta) = (1, 0)$ ; an intermediate viscous case,  $(\alpha, \beta) = (3, 0)$ ; and a case approaching that of Coulomb plastic,  $(\alpha, \beta) = (30, 1)$ . Figure 6a shows the topographic forms using the mass balance and taking the positive sign in (30). From the analytical solutions for these rheologies (25), the exponents characterizing the topographic profiles are 1/3, 3/7, and 30/31, respectively. The validity of neglecting the mass balance pattern in deriving these exponents is confirmed by the profiles, which are almost indistinguishable from the analytical forms. This is confirmed by comparing profiles with opposite mass balance patterns (i.e., using different signs in (30)), as shown in Figure 6b. The two profiles differ by less than 20 m, with differences largest near the divide and when the linear viscous rheology is used.

[51] To further illustrate the insensitivity of the topographic form to the mass balance, Figure 7 shows orogen profiles calculated with an imposed a 2 km-wide top-hat “spike” in the mass balance in the middle the orogen. The

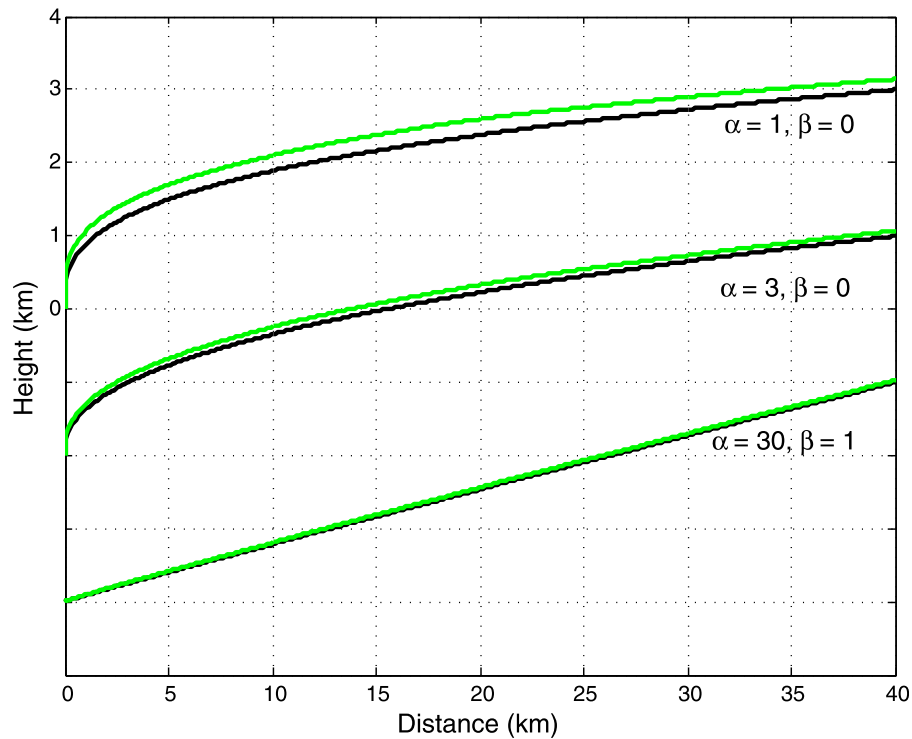


**Figure 7.** For different rheologies, the response of the critical form to adding a large ( $20 \text{ cm yr}^{-1}$ ) spike in rock uplift rates in a 2 km wide swath centered at 20 km. The black shows the critical form for the control case; the gray line shows the critical form including the spike in mass balance. Curves are offset on the  $y$  axis for clarity. Even with this large perturbation to the mass balance there is relatively little change in the critical form. As in Figure 6, near Coulomb plastic rheologies are the least sensitive.

amplitude of this imposed spike is  $20 \text{ cm yr}^{-1}$ , or in other words, one hundred times the average rock uplift rates. The spike has its biggest effect on the profile at the point where it is imposed, but even for a linear viscous rheology, the maximum difference between the profiles is less than 200 m. For the case of  $\alpha, \beta = (30, 1)$ , the maximum difference is 30 m.

[52] Figures 6b and 7 demonstrate a profound insensitivity of the topographic form to the mass balance, an insensitivity that increases with increasing  $\psi$ . The reasons are twofold. Firstly, as argued by *Emerman and Turcotte* [1983] and in section 4.2, the flux of material through the orogen is dominated by two terms, the translational flux and the deformation flux, which are both much larger in magnitude than typical values of the local mass balance. Secondly, even if spatial variations in mass balance are enough to significantly affect  $F(x)$ , (19) is a nonlinear diffusion equation. Therefore, large changes in  $F(x)$  can be balanced by only a small change in the shape of the orogen profile (i.e., either  $h$  or  $dz_s/dx$ ), because each of these two terms is raised to a large power in (19).

[53] In the context of orogen development, the insensitivity of the orogen profile to precipitation patterns is demonstrated by the numerical modeling of *Stolar et al.* [2007]. There is a parallel with glaciology because ice is also a power law viscous fluid. The rheology of ice is typically given by  $\alpha = 3$  and  $\beta = 0$  in (13). *Boudreaux and Raymond* [1997] and *Roe* [2002] showed that the profiles

of glaciers and ice sheets are extremely insensitive to the pattern of the mass balance. *Roe* [2002] derived the solution for the response of an ice sheet profile to a  $\delta$  function spike in the accumulation pattern. This solution can be adapted to the wedge problem considered here by incorporating the basal traction term. One result from the earlier study is that an ice sheet profile is most sensitive when the  $\delta$ -function is close to the center of the ice sheet, where the surface slope is small. The reason can also be seen from (19): the smaller the surface slope, the greater the adjustment in the thickness to balance a perturbation in the flux.

[54] Lastly, we note that because high exponents in the power law rheology allow  $h$  and  $dz_s/dx$  to effectively adjust to perturbations, the orogen will also be insensitive to the specific values used for the model parameters that appear in (19) at the same order as the mass balance. Large changes in the flow factor  $A$  or in the normalizing stress  $\tau^*$  would be required to cause significant changes in the topographic form.

[55] So far we have considered the basal velocity,  $u_b$ , to be uniform. However, in reality it will depend on the details of how material is incorporated into the orogenic wedge whether by frontal accretion or underplating [e.g., *Willett*, 2001]. For example, if underplating into the wedge is uniform, the depth of the layer of crustal material scraped off the subducting plate and subsumed into the wedge must vary across the orogen [e.g., *Willett*, 2001, Figure 4], which

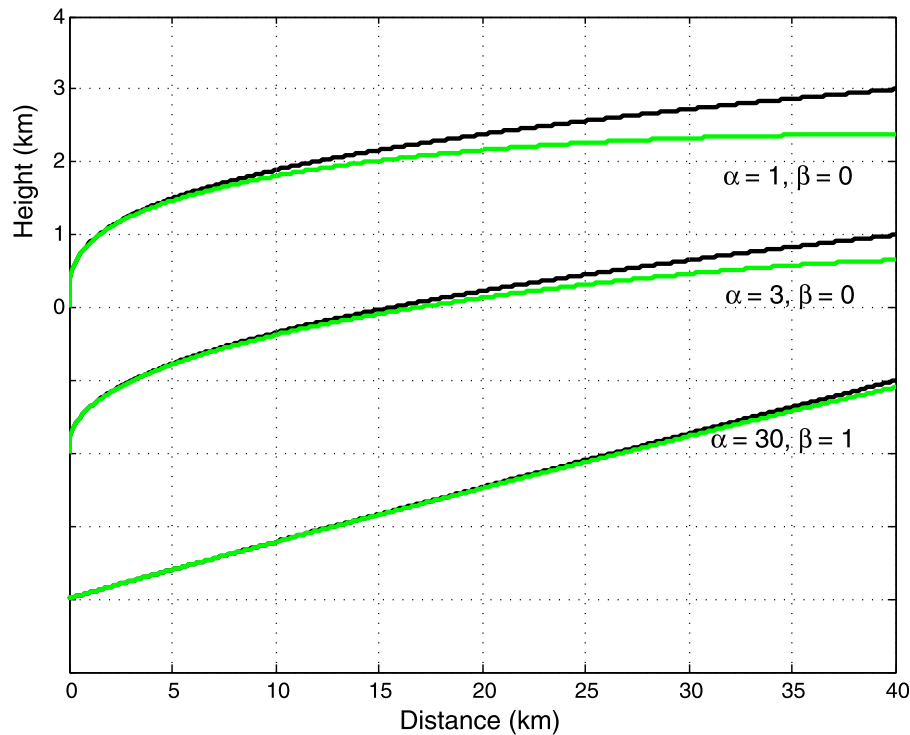


**Figure 8.** For different rheologies, the response of the critical form to changing the pattern of the basal traction velocity from constant (black lines) to a linear decrease (gray lines). Curves are offset on the  $y$  axis for clarity. The surface slope at the divide must go to zero. For a near Coulomb plastic rheology, the critical form is almost unaffected.

will affect how the traction stresses from the subducting slab are transferred to the base of the wedge.

[56] The numerical solution of (19) allows for  $u_b$  to be specified as a function of position. To illustrate the effect of spatial variations in  $u_b$ , we consider a simple linear decrease across the wedge:  $u_b(x) = u_b^*(1 - x/L)$ , where  $u_b^*$  is a constant. From (19), if  $u_b$  goes to zero at the divide, the surface slope must go to zero there. Figure 8 shows this clearly happening in the linear viscous case. However, as the exponent in the power law rheology increases, the spatial pattern in  $u_b$  has decreasing influence on the topographic form. Substituting  $u_b(x)$  into (22), it can be rearranged to show that  $dz_s/dx \propto (1 - x/L)^{1/\alpha}$  which, for higher powers of  $\alpha$ , and except in the vicinity of  $x \sim L$ , is nearly constant.

## 7. Approach to a Plateau

[57] At depth, higher temperatures means deformation occurs more readily. For larger orogens and plateaux, thermal weakening of the crustal root becomes an important factor in their development [e.g., *Stüwe*, 2002]. The power law rheology in (13) can be adapted to qualitatively explore how this affects the topographic form.

[58] Our goal here is only illustrative, and so there is some flexibility in how to represent this depth-dependent behavior. For example, an Arrhenius-type function can be introduced into the flow factor:  $A \sim \exp(Q/RT)$ , where  $Q$  is an activation energy and  $T$  is the temperature. For our purposes, it also suffices to specify a depth dependence to the normalizing stress,  $\tau^*$ : the lower  $\tau^*$ , the more readily

the crust deforms. To demonstrate the effect of different rheologies for the upper and lower crust,  $\tau^*$  is only changed below a given depth,

$$\begin{aligned} \tau^* &= \tau_0^* & (z - z_s) < H_t \\ \tau^* &= \tau_0^* e^{-\frac{(z - z_s) - H_t}{\Delta H}} & (z - z_s) \geq H_t \end{aligned} \quad (31)$$

where  $\tau_0^*$  is constant. We take  $H_t = 25$  km, and  $\Delta H = 2$  km. In an Arrhenius-type temperature dependence, this short  $e$ -folding scale would correspond approximately to a  $Q$  of  $135 \text{ kJ mol}^{-1}$  and a geothermal gradient of  $20 \text{ K km}^{-1}$ .

[59] Figure 9a show the height of the orogen for three different rheologies, as a function of orogen width and calculated from the numerical solution. It becomes increasingly hard to build the profile above about 4 km in height (or 25 km in total depth): the strong decrease in  $\tau^*$  means steep surface slopes cannot be supported at depth, and so the orogen profile flattens out.

[60] The results in this paper have presented the strength of the tectonic feedback in terms of  $\psi$ , the exponent governing the critical topographic form. An equivalent value for  $\psi$  for the curves in Figure 9a can be calculated from the slope of  $\ln(H)/\ln(L)$ . These are shown in Figure 9b. For small orogen widths,  $\psi$  is a constant and, as expected, matches the values from the analytical solutions. As the orogen profile nears 4 km in height, however, the flattening out of the profile is reflected in a steep drop in the value of  $\psi$ . For the near Coulomb plastic case of  $(\alpha, \beta) = (30, 1)$ , this drop in  $\psi$  occurs over a change in width of only 20 km. During this transition,

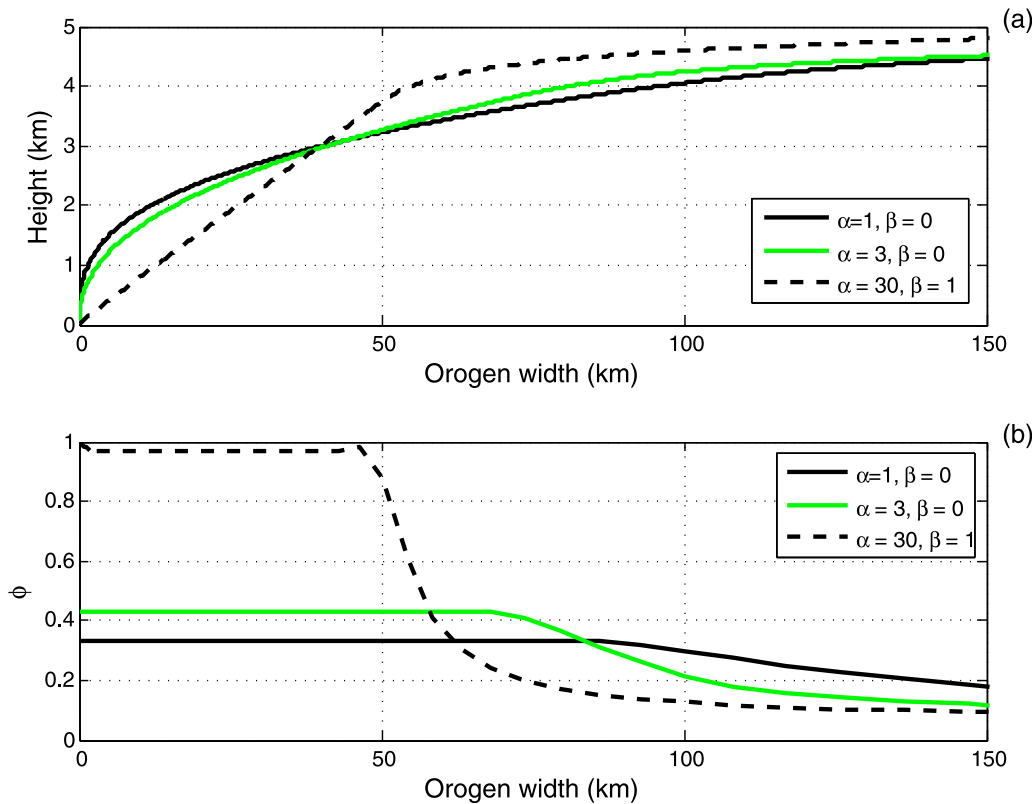


**Figure 9.** For different rheologies, (a) height of the orogen  $H$  and (b) value of the height-width power law relationship  $\psi$  as a function of orogen scale  $L$  during the approach to a plateau. An exponential decrease in the normalizing stress has been assumed at depths exceeding 25 km. Consequently shear stresses within the orogen cannot support topography above approximately 4 km. See equation (31) and text for more details.

there is an accompanying large change in orogen sensitivity and feedback strength, which can be calculated from (29), and is shown in Figure 10. For the more viscous rheologies, the transition is more gradual.

## 8. Discussion

[61] A framework has been presented to evaluate the importance of precipitation and accretionary flux in setting the scale and erosion rates of steady state convergent orogens. The rheologic control on the orogen is directly manifested in the relationship between the height and width. A given rheology results in a topographic form for the orogen, which can be combined with fluvial erosion to produce scaling relationships for the width, height, and rock uplift rates of the orogen in terms of the accretionary flux,  $F$ , and precipitation rate,  $P$ . Whereas previous studies considered only Coulomb plastic wedges with a critical taper angle, we have extended the analysis to incorporate rheologies varying from linear viscous to Coulomb plastic. Orogen development can be reduced to a straightforward flux-balance problem. The growth or decay of the orogen is proportional to the imbalance between the accretionary and erosional fluxes, and the system is constrained to always have the same critical topographic form.

[62] There are two principal results. The first is that for a wide range of assumed rheologies, the topographic form is

strongly insensitive to the pattern of erosion rates and underplating, just as in the case of a critical taper wedge. The tectonic governor concept is derived from the fact that regardless of rheology, a wedge will tend to form steady. An additional conclusion is that the sensitivity of the orogen width to precipitation and accretionary flux remains similar regardless of rheology. The exponents on  $F$  and  $P$  in the scaling relationships vary by less than a factor of two for all common choices of the erosion parameters. The exponents in the scaling relationships are also all less than one, implying a generally weak sensitivity of orogen attributes to changes in climate or tectonic forcing.

[63] The vertically integrated horizontal mass flux within the orogen is composed of a translational component due to the basal traction and an oppositely directed deformational component. This deformational flux can be viewed as a return flow directed toward to the front of the wedge. It operates as a strongly nonlinear diffusion process that, given a perturbation, will restore the wedge back to a steady state form. Significant perturbations to the critical topographic form are therefore only possible during the transient evolution of the system, and then only by changes occurring on timescales that are shorter than that required for the deformational flux to adjust. This timescale can be estimated by a scale analysis of (19) and (20). The timescale for the restoration by the deformational flux is shorter with increasing  $\psi$ . The prediction is that Coulomb plastic wedges should return



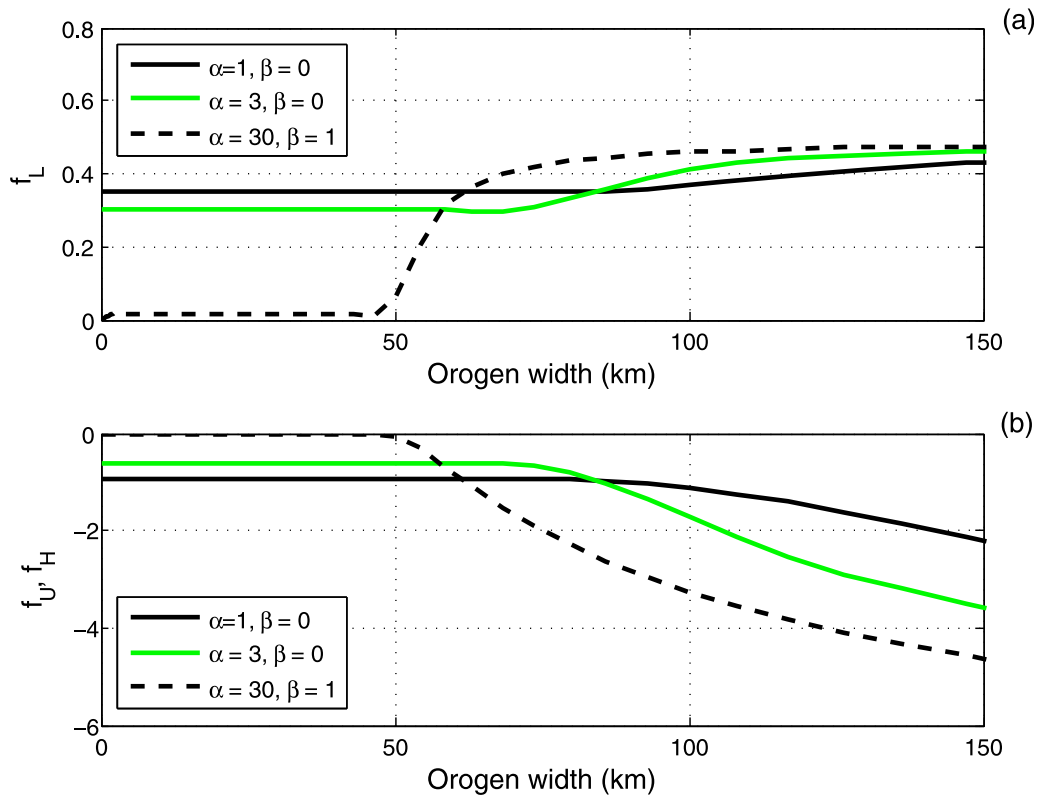


**Figure 10.** For different rheologies, feedback factors (a)  $f_L$  and (b)  $f_H$  and  $f_U$ , as a function of orogen size  $L$ , during the approach to a plateau.  $(h, m, n) = (2, 1/2, 1)$  was assumed for the values shown. Details of calculations as for Figure 9. Because  $hm/n = 1$ ,  $f_H = f_U$ , but this is not generally true. Note the different scales on the y axes. For the near-Coulomb plastic rheology, note the strong change in orogen sensitivity between approximately 50 and 70 km in width.

to a steady state (or critical) form faster than a linear viscous wedge.

[64] The strongly restorative nature of this nonlinear diffusion process suggests that the conclusions of this study should be robust with respect to the abstraction and assumptions used in the analysis. Our analysis shows that an orogenic wedge will tend to maintain a critical form as long as there is sufficient accretion and erosion to allow the system to move between different critical forms if the effective rheology changes with wedge size. All that is required is some tendency of the wedge to grow or shrink laterally as it grows or shrinks vertically.

[65] We have assumed erosion occurs fluvially and via a standard formulation of river incision into bedrock. Recent work has explored alternative “tools-and-cover” formulations [Sklar and Dietrich, 1998, 2001; Whipple and Tucker, 2002], which reflect the effects of varying sediment concentrations on the erosive ability of the river. N. M. Gasparini and M. T. Brandon (A power law scaling relationship for bedrock incision at the drainage network scale, submitted to *Journal of Geophysical Research*, 2010) argue that such models can all be characterized by effective values of  $m$  and  $n$ . This result indicates that our analysis here can be easily expanded to include a range of fluvial incision models. Tomkin and Roe [2007] have explored the case of glacial erosion; they argue a fully glaciated orogen is more sensitive to precipitation than the fluvial case, and this conclusion would carry over to the present analysis. Whatever the

dominant processes are in reality, the scaling relationships demonstrate that the general dependence of erosion on slope and drainage area are important, and suggest that overly simplistic treatments such as purely diffusive erosion, or buzz-sawing an orogen above a given altitude will not properly model the system dynamics.

[66] Further development of the model rheology is possible. Apart from the depth dependence of the normalizing stress, the rheology has been assumed homogenous within the orogen. The exponent on the power law (13) might also be varied with depth or horizontal distance to provide, for example, a mixed plastic-viscous rheology. Crustal deformation along localized shear zones, whether brittle or viscous, has been neglected. However, they are pinned to material and thus are advected rearward into the wedge (as can be seen in sandbox experiments including erosion [e.g., Konstantinovskia and Malavieille, 2005]). Although no material motion across faults can take place, the location of active faults must step outward in order to produce an inward flux of material to balance the surface erosion occurring within the orogen. Sand box experiments with surface erosion included show material trajectories that are similar to those in idealized Coulomb plastic wedges [e.g., Hoth et al., 2006; Brandon et al., 1998], and numerical models that do not have faults but do have zones of concentrated deformation closely follow our analytical results [Stolar et al., 2006, 2007]. Using numerical models, Stockmal et al. [2007] find agreement with wedge predictions at the large scale, and explore departures at

the local scale associated with individual thrusts. It is unlikely therefore that the inclusion of faults would overturn the general picture developed here; however, further work in this area would clearly be useful.

[67] We have only considered steady state balances. *Whipple and Meade* [2006] and *Stolar et al.* [2006] show in analytical and numerical models that the transient evolution of the system occurs in a quasi steady state fashion [e.g., *Kooi and Beaumont*, 1996] in which the critical form is maintained at all times, but that the rate of growth (or decay) of volume is proportional to the flux imbalance between the accretionary and erosional fluxes. *Whipple and Meade* [2006] and *Roe et al.* [2008] show further that the characteristic timescale to steady state is a function of the exponents in the scaling relationship. These results translate directly to the rheologies considered here. A dynamical system can have several relevant timescales [e.g., *Willett and Brandon*, 2002]. In addition to the “volume-filling” timescale noted above, the viscous rheologies also can be characterized by kinematic timescale (due to advection), and a diffusive timescale (due to deformation), directly analogous to the situation for sliding glaciers [e.g., *Nye*, 1965; *van de Wal and Oerlemans*, 1995; *Bahr et al.*, 1998]. Our focus in this study was on steady state relationships, but these transient dynamics as a function of rheology are tractable and interesting issues to pursue.

[68] Only one-sided orogens have been considered. Two additional constraints allow the two-sided case to be constructed out of back-to-back one-sided wedges (following *Whipple and Meade* [2004]). Continuity requires the two wedges to have the same height, and conservation of mass means that the sum of the fluxes accommodated under each of the wedge equals the total incoming accretionary flux. The pattern of strain within the orogen will depend sensitively on the pattern of underplating assumed [e.g., *Willett*, 1999a, 2001]. However since the critical topographic form is so insensitive to the pattern of underplating and erosion, the scaling relationships will be essentially the same. This has been demonstrated for the Coulomb plastic rheology [e.g., *Whipple and Meade*, 2004; *Roe et al.*, 2008], and the extension to the present study is direct.

## Appendix A: Feedback Factors and Gains

[69] In deriving the expressions for the feedback factors and gains, we follow the analysis of *Roe et al.* [2008] where more details of this standard method can be found. We can define sensitivity parameters for  $L$ ,  $H$ , and  $U$ , which relate a change in these variables to a change in the accretionary flux,

$$\begin{aligned}\Delta L &= \lambda_L \Delta F \\ \Delta H &= \lambda_H \Delta F \\ \Delta U &= \lambda_U \Delta F\end{aligned}\quad (A1)$$

Obviously, these sensitivity factors are different when a feedback is operating compared to when it is not. The gains and feedback factors characterize this change in sensitivity of the system.

[70] To begin with, the orogenic wedge system obeys the scaling relationship from (9),

$$F \propto L^{1+hm-n} H^n P^m. \quad (A2)$$

We define the reference case as the Coulomb critical wedge:  $H \propto L$ . A truncated Taylor series expansion of (A2) gives

$$\Delta F = \frac{\partial F}{\partial L} \Delta L + \frac{\partial F}{\partial H} \Delta H = \frac{\partial F}{\partial L} \Delta L + \frac{\partial F}{\partial H} \frac{\partial H}{\partial L} \Delta L, \quad (A3)$$

which on substitution from (A2) and assuming  $H \propto L$ , gives

$$\Delta F = \left\{ (1 + hm - n) \frac{F}{L} + n \frac{F}{H} \frac{H}{L} \right\} \Delta L. \quad (A4)$$

And so for the reference case (denoted by the superscript 0)

$$\lambda_L^0 = \frac{1}{(1 + hm)} \frac{L}{F}. \quad (A5)$$

In the general case however,  $H \propto L\psi$ . On substitution of this into (A2) and (A3), we get

$$\begin{aligned}\Delta F &= \left\{ (1 + hm) \frac{F}{L} + n(\psi - 1) \frac{F}{L} \right\} \Delta L \\ &= \frac{1}{\lambda_L^0} \left\{ 1 + \lambda_L^0 n(\psi - 1) \right\} \frac{F}{L} \Delta L.\end{aligned}\quad (A6)$$

Therefore, for this general case

$$\lambda_L = \frac{\lambda_L^0}{1 - \frac{n(1-\psi)}{(1+hm)}}. \quad (A7)$$

The gain,  $G_L$ , is defined as  $\Delta L/\Delta L_0$ , and so is equal to  $\lambda_L/\lambda_L^0$ . The feedback factor is defined via  $G_L = 1/(1 - f_L)$ , and so from (A7) is given by

$$f_L = \frac{n(1 - \psi)}{1 + hm}. \quad (A8)$$

For  $\lambda_H$ , the Taylor series expansion of (A2) can be written in terms of  $\Delta H$ ,

$$\Delta F = \left\{ \frac{\partial F}{\partial H} + \frac{\partial F}{\partial L} \frac{\partial L}{\partial H} \right\} \Delta H \quad (A9)$$

The reference case  $\lambda_H^0$  has a similar form to that for orogen width,

$$\lambda_H^0 = \frac{1}{(1 + hm)} \frac{H}{F} \quad (A10)$$

On substituting the critical form  $L = H^{1/\psi}$  into (A9), and following the method above, we get

$$f_H = \frac{(\psi - 1)(1 + hm - n)}{\psi(1 + hm)}. \quad (A11)$$

The rock uplift rate is related to  $F$  and  $L$  via  $U = F/L$ . *Roe et al.* [2008] showed that the following relationship always holds,

$$G_U = \frac{1 + hm - G_L}{hm}. \quad (A12)$$

Upon substitution from (A8) and a lot of rearranging, this boils down to

$$f_U = \frac{n(\psi - 1)}{(1 + hm)[hm - n(1 - \psi)]}. \quad (\text{A13})$$

## Appendix B: Coordinate Stretching

[71] A horizontal coordinate transformation can be used to remove numerical problems encountered in integrating (19) to calculate the critical topographic form when no analytical solution is possible. Simplified, (19) has the following form,

$$z_s^\nu \frac{dz_s^\mu}{dx} = c_1 z_s + c_2 F(x), \quad (\text{B1})$$

where  $c_1$ ,  $c_2$  are constants, and  $\nu = \alpha(1 - \beta) + 2$ , and  $\mu = \alpha$ .

[72] The boundary condition is that  $z_s = 0$  at  $x = 0$ . For finite  $F(x = 0)$ , and for finite  $\alpha$ , this means  $dz_s/dx$  must go to infinity at  $x = 0$ . The goal is to find a coordinate transform  $t = t(x)$  that keeps the slope  $dz_s/dt$  well behaved at that point. First, we construct the series solution for  $z_s$  in the neighborhood of  $x = 0$ ,

$$z_s = x^p (a_0 + a_1 x + a_2 x^2 + \dots), \quad (\text{B2})$$

where  $a_n$  are constants to be found, and the first term in the series is of order  $p$ , also to be found. Taking the derivative gives

$$\frac{dz_s}{dx} = x^{p-1} (a_0 p + a_1 (p+1)x + a_2 (p+2)x^2 + \dots). \quad (\text{B3})$$

On substitution of these series expansions into (B1), the leading order terms on the left- and right-hand side must match. So for finite  $F(x = 0)$ , we must have

$$p\nu + (p-1)\mu = 0, \quad (\text{B4})$$

or

$$p = \frac{\mu}{\mu + \nu}. \quad (\text{B5})$$

Therefore in the limit of  $x \rightarrow 0$ ,  $z_s \sim x^{\frac{\mu}{\mu+\nu}}$  and so  $dz_s/dx \sim x^{-\frac{\mu}{\mu+\nu}}$ . In the case of a linear viscous wedge  $(\alpha, \beta) = (1, 0)$ , which gives  $(\mu, \nu) = (3, 1)$ , and so  $dz_s/dx \sim x^{-\frac{3}{4}}$ .

[73] The solution for the orogen profile is just

$$z_s(x) = \int_0^x \left( \frac{dz_s}{dx} \right) dx. \quad (\text{B6})$$

The forgoing analysis shows that this is an improper integral with an integrable power law singularity at the lower boundary. For such an integral, if the integrand,  $f(x)$ , diverges as  $(x - a)^{-\gamma}$ ,  $0 \leq \gamma < 1$ , near  $x = a$ , the standard identity is [e.g., *Press et al.*, 1992],

$$\int_a^b f(x) dx = \frac{1}{1-\gamma} \int_0^{(b-a)^{1-\gamma}} t^{\frac{\gamma}{1-\gamma}} f\left(t^{\frac{1}{1-\gamma}} + a\right) dt. \quad (\text{B7})$$

Therefore we use the change of variable  $t = x^{1-\frac{\mu}{\mu+\nu}}$ , before numerically integrating to solve for the orogen profile.

[74] **Acknowledgments.** We thank Philip Roe, Drew Stolar, Sean Willett, Hugh Sinclair, and Peter Molnar for insightful conversations and the crew of the *Mama Dina* for looking after us. G.H.R. acknowledges support from NSF Continental Dynamics 6312293, and M.T.B. acknowledges support from NSF EAR-0447140 and NSF Continental Dynamics 0208652.

## References

- Bahr, D. B., W. T. Pfeffer, C. Sassoloas, and M. F. Meier (1998), Response time of glaciers and a function of size and mass balance: 1. Theory, *J. Geophys. Res.*, 103(B5), 9777–9782, doi:10.1029/98JB00507.
- Batchelor, G. K. (2000), *An Introduction to Fluid Dynamics*, 635 pp., Cambridge Univ. Press, Cambridge, U. K.
- Beaumont, C., P. Fullsack, and J. Hamilton (1992), Erosional control of active compressional orogens, in *Thrust Tectonics*, edited by K. R. McClay, pp. 1–18, Chapman Hall, New York.
- Beaumont, C., H. Kooi, and S. D. Willett (2000), Progress in coupled tectonic - surface process models with applications to rifted margins and collisional orogens, in *Geomorphology and Global Tectonics*, edited by M. Summerfield, pp. 29–56, John Wiley, Chichester, U. K.
- Boudreaux, A., and C. F. Raymond (1997), Geometry response of glaciers to changes in spatial pattern of mass balance, *Ann. Glaciol.*, 25, 407–411.
- Brandon, M. T., M. K. Roden-Tice, and J. I. Garver (1998), Late Cenozoic exhumation of the Cascadia accretionary wedge in the Olympic Mountains, northwest Washington State, *Geol. Soc. Am. Bull.*, 110, 985–1009.
- Buck, W. R., and D. Sokoutis (1994), Analogue model of gravitational collapse and surface extension during continental convergence, *Nature*, 369, 737–740.
- Chapple, W. M. (1969), Fold Shape and Rheology: The folding of an isolated viscous plastic layer, *Tectonophysics*, 7, 97–116.
- Chapple, W. M. (1978), Mechanics of thin-skinned fold-and-thrust belts, *Geol. Soc. Am. Bull.*, 89, 1189–1198.
- Cowan, D. S., and R. M. Silling (1978), A dynamic scaled model of accretion at trenches and its implications for the tectonic evolution of subduction complexes, *J. Geophys. Res.*, 83(B11), 5389–5396, doi:10.1029/JB083iB11p05389.
- Dahlen, F. A. (1984), Noncohesive critical Coulomb wedges: An exact solution, *J. Geophys. Res.*, 89(B12), 125–133, doi:10.1029/JB089iB12p10125.
- Dahlen, F. A. (1990), Critical taper model of fold-and-thrust belts and accretionary wedges, *Annu. Rev. Earth Planet. Sci.*, 18, 55–99.
- Davis, D., J. Suppe, and F. A. Dahlen (1983), Mechanics of fold-and-thrust belts and accretionary wedges, *J. Geophys. Res.*, 88(B2), 1153–1172, doi:10.1029/JB088iB02p01153.
- Elliott, D. (1976), The motion of thrust sheets, *J. Geophys. Res.*, 81(5), 949–963, doi:10.1029/JB081i005p00949.
- Ellis, S., P. Fullsack, and C. Beaumont (1995), Oblique convergence of the crust driven by basal forcing: implications for length-scales of deformation and strain partitioning in orogens, *Geophys. J. Int.*, 120, 24–44.
- Emerman, S. H., and D. L. Turcotte (1983), A fluid model for the shape of accretionary wedges, *Earth Planet. Sci. Lett.*, 63, 379–384.
- England, P. (1983), Constraints on extension of continental lithosphere, *J. Geophys. Res.*, 88(B2), 1145–1152, doi:10.1029/JB088iB02p01145.
- England, P., and D. P. McKenzie (1982), A thin viscous sheet model for continental deformation, *Geophys. J. R. Astron. Soc.*, 70, 295–321. (Correction, *Geophys. J. R. Astron. Soc.*, 73, 523–532, 1983.)
- England, P., G. Houseman, and L. Sonder (1985), Length scales for continental deformation in convergent, divergent, and strike-slip environments: analytical and approximate solutions for a thin viscous sheet model, *J. Geophys. Res.*, 90(B5), 4797–4810, doi:10.1029/JB090iB05p03551.
- Glen, J. W. (1955), The creep of polycrystalline ice, *Proc. R. Soc., Ser. A*, 228, 519–538.
- Hack, J. T. (1957), Studies of longitudinal stream profiles in Virginia and Maryland, *U.S. Geol. Surv. Prof. Pap.*, 294-B, 45–97.
- Hilley, G. E., and M. Strecker (2004), Steady state erosion of critical coulomb wedges with applications to Taiwan and the Himalaya, *J. Geophys. Res.*, 109, B01411, doi:10.1029/2002JB002284.
- Hilley, G. E., M. Strecker, and V. A. Ramos (2004), Growth and erosion of fold-and-thrust belts with an application to the Aconcagua Fold and Thrust Belt, Argentina, *J. Geophys. Res.*, 109, B01410, doi:10.1029/2002JB002282.
- Hoth, S., J. Adam, N. Kukowshi, and O. Oncken (2006), Influence of erosion on the kinematics of bivergent orogens: results from scaled sandbox simulations, in *Tectonics, Climate, and Landscape Evolution, Penrose Conf. Ser.*, vol. 398, edited by S. D. Willett et al., pp. 201–225, Geol. Soc. of Am., Boulder, Colo.
- Howard, A. D. (1980), Thresholds in river regime, in *The Concept of Geomorphic Thresholds*, edited by D. R. Coates and J. D. Vitek, pp. 227–258, chap. 11, Allen and Unwin, Boston, Mass.

- Howard, A. D., M. A. Seidl, and W. E. Dietrich (1994), Modeling fluvial erosion on regional to continental scales, *J. Geophys. Res.*, *99*(B7), 13,971–13,986, doi:10.1029/94JB00744.
- Hutter, K. (1983), *Theoretical Glaciology*, D. Reidel, Dordrecht, Holland.
- Konstantinovskia, E., and J. Malavieille (2005), Erosion and exhumation in accretionary orogens: experimental and geological approaches, *Geochem. Geophys. Geosyst.*, *6*, Q02006, doi:10.1029/2004GC000794.
- Kooi, H., and C. Beaumont (1996), Large-scale geomorphology: classical concepts reconciled and integrated with contemporary ideas via a surface processes model, *J. Geophys. Res.*, *101*(B2), 3361–3386, doi:10.1029/95JB01861.
- Maxwell, J. C. (1868), On governors, *Proc. R. Soc., Ser. A*, *16*, 270–283.
- Montgomery, D. R., and W. E. Dietrich (1992), Channel initiation and the problem of landscape scale, *Science*, *255*, 826–830.
- Norton, F. H. (1929), *Creep of Steel at High Temperature*, McGraw-Hill, New York.
- Nye, J. F. (1965), The frequency response of glaciers, *J. Glaciol.*, *5*, 567–587.
- Paterson, W. S. B. (1994), *The Physics of Glaciers*, 3rd ed., 480 pp., Pergamon, Oxford, U. K.
- Pollard, D. D., and R. C. Fletcher (2005), *Fundamentals of Structural Geology*, 500 pp., Cambridge Univ. Press, Cambridge, U. K.
- Press, W. H., B. P. Flannery, S. A. Teukolsky, and W. T. Vetterling (1992), *Numerical Recipes: The Art of Scientific Computing*, 933 pp., Cambridge Univ. Press, New York.
- Price, R. A. (1973), Large-scale gravitational flow of supracrustal rocks, southern Canadian Rockies, in *Gravity and Tectonics*, edited by K. A. De Jong and R. Scholten, pp. 491–502, John Wiley, New York.
- Roe, G. H. (2002), Modeling orographic precipitation over ice sheets: An assessment over Greenland, *J. Glaciol.*, *48*, 70–80.
- Roe, G. H. (2005), Orographic precipitation, *Annu. Rev. Earth Planet. Sci.*, *33*, 645–671.
- Roe, G. H. (2009), Feedbacks, timescales, and seeing red, *Annu. Rev. Earth Planet. Sci.*, *37*, 93–115.
- Roe, G. H., D. R. Montgomery, and B. Hallet (2003), Orographic precipitation and the relief of mountain ranges, *J. Geophys. Res.*, *108*(B6), 2315, doi:10.1029/2001JB001521.
- Roe, G. H., D. Stolar, and S. D. Willett (2006), The sensitivity of a critical wedge orogen to climatic and tectonic forcing, in *Tectonics, Climate, and Landscape Evolution*, vol. 398, edited by S. D. Willett et al., pp. 227–239, Geol. Soc. of Am., Boulder, Colo.
- Roe, G. H., K. X. Whipple, and J. K. Fletcher (2008), Feedbacks between climate, erosion, and tectonics in a critical wedge orogen, *Am. J. Sci.*, *308*, 815–842.
- Routledge, R. (1900), *Discoveries and Inventions of the Nineteenth Century*, 13th ed., Routledge, London. (Available on Wikipedia commons)
- Sinclair, H. D., M. Gibson, M. Naylor, and R. G. Morris (2005), Asymmetric growth of the Pyrenees revealed through measurement and modeling of orogenic fluxes, *Am. J. Sci.*, *305*, 369–406.
- Sklar, L. S., and W. E. Dietrich (1998), River longitudinal profiles and bedrock incision models: Stream power and the influence of sediment supply, in *Rivers Over Rock: Fluvial Processes in Bedrock Channels*, edited by K. Tinkler and E. E. Wohl, pp. 237–260, AGU, Washington, D. C.
- Sklar, L. S., and W. E. Dietrich (2001), Sediment and rock strength controls on river incision into bedrock, *Geology*, *29*, 1087–1090.
- Smith, R. B. (1975), Unified theory of onset of folding, boudinage, and mullion structure, *Geol. Soc. Am. Bull.*, *86*, 1601–1609.
- Smith, R. B. (1977), Formation of folds, boudinage, and mullions in non-Newtonian materials, *Geol. Soc. Am. Bull.*, *88*, 312–320.
- Stockmal, G. S., C. Beaumont, M. Nguyen, and B. Lee (2007), Mechanics of thin-skinned fold-and-thrust belts: Insights from numerical models, in *Whence the Mountains? Inquires Into the Evolution of Orogenic Systems: A Volume in Honor of Raymond A. Price*, vol. 433, edited by J. W. Sears et al., pp. 63–98, Geol. Soc. of Am., Boulder, Colo.
- Stolar, D. R., S. D. Willett, and G. H. Roe (2006), Evolution of a critical orogen under various forcing scenarios: findings from a numerical sandbox, in *Tectonics, Climate, and Landscape Evolution*, vol. 398, edited by S. D. Willett et al., pp. 240–250, Geol. Soc. of Am., Boulder, Colo.
- Stolar, D. R., G. H. Roe, and S. D. Willett (2007), Controls on the patterns of topography and erosion rate in a critical orogen at steady state, *J. Geophys. Res.*, *112*, F04002, doi:10.1029/2006JF000713.
- Stüwe, K. (2002), *Geodynamics of the Lithosphere*, 449 pp., Springer, Berlin.
- Tomkin, J. T., and G. H. Roe (2007), Climate and tectonic controls on glaciated critical taper orogens, *Earth Planet. Sci. Lett.*, *262*, 385–397.
- van de Wal, R. S. W., and J. Oerlemans (1995), Response of valley glaciers to climate change and kinematic waves: A study with a numerical ice-flow model, *J. Glaciol.*, *9*, 115–131.
- Whipple, K. X. (2004), Bedrock rivers and the geomorphology of active orogens, *Annu. Rev. Earth Planet. Sci.*, *32*, 151–185.
- Whipple, K. X. (2009), The influence of climate on the tectonic evolution of mountain belts, *Nat. Geosci.*, *2*, 97–104.
- Whipple, K. X., and B. J. Meade (2004), Dynamic coupling between erosion, rock uplift, and strain partitioning in two-sided, frictional orogenic wedges at steady state: An approximate analytical solution, *J. Geophys. Res.*, *109*, F01011, doi:10.1029/2003JF000019.
- Whipple, K. X., and B. J. Meade (2006), Orogen response to changes in climatic and tectonic forcing, *Earth Planet. Sci. Lett.*, *243*, 218–228.
- Whipple, K. X., and G. Tucker (2002), Implications of sediment-flux dependent river incision models for landscape evolution, *J. Geophys. Res.*, *107*(B2), 2039, doi:10.1029/2000JB000044.
- Whipple, K. X., E. Kirby, and S. H. Brocklehurst (1999), Geomorphic limits to climate-induced increases in topographic relief, *Nature*, *401*, 39–43.
- Willett, S. D. (1999a), Orogeny and orography: The effects of erosion on the structure of mountain belts, *J. Geophys. Res.*, *104*(B12), 28,957–28,981, doi:10.1029/1999JB900248.
- Willett, S. D. (1999b), Rheological dependence of extension in viscous and plastic wedge models of convergent orogens, *Tectonophysics*, *305*, 419–435.
- Willett, S. D. (2001), Uplift, shortening, and steady state topography in active mountain belts, *Am. J. Sci.*, *301*, 455–485.
- Willett, S. D., and M. T. Brandon (2002), On steady states in mountain belts, *Geology*, *30*(2), 175–178.
- Willett, S. D., F. Schlunegger, and V. Picotti (2006), Messinian climate change and erosional destruction of the central European Alps, *Geology*, *34*, 613–616.

M. T. Brandon, Department of Geology and Geophysics, Yale University, New Haven, CT 06520, USA.

G. H. Roe, Department of Earth and Space Sciences, University of Washington, Seattle, WA 98195, USA. (gerard@ess.washington.edu)